

# Analysis of windowing/leakage effects in frequency response function measurements<sup>☆</sup>

J. Schoukens\*, Y. Rolain, R. Pintelon

*Department ELEC, Vrije Universiteit Brussel, Pleinlaan 2, B1050 Brussels, Belgium*

Received 24 June 2004; received in revised form 23 February 2005; accepted 10 August 2005

Available online 30 September 2005

## Abstract

This paper analyses the errors on the frequency response function measurement of a transfer function due to finite window effects (leakage). First an analysis of the rectangular and the Hanning window is made. It will be shown that the leakage error consists of two components: a transient error due to initial and end condition effects, and an interpolation error due to the combination of neighbouring spectral lines. Starting from these insights an extremely simple expression to calculate the leakage induced bias and variance errors is generated. Eventually, a new ‘default’ window is proposed with slightly better properties. This allows a reduction in measurement time by 25% if the leakage errors dominate the disturbing output noise.

© 2005 Elsevier Ltd. All rights reserved.

*Keywords:* Leakage; Windows; Frequency response function

## 1. Introduction

Frequency response function measurements of transfer functions (FRF) are very intensively used in many engineering fields. Nowadays these measurements are mostly done with the discrete Fourier transform (DFT), calculated with the fast Fourier transform (FFT). The DFT calculates the spectrum of the time domain sequence on a discrete equidistant set of frequencies, called spectral lines. For random excitations these spectral results are disturbed by leakage (windowing) errors that are induced by the finite length of the measurement window; the signal at one frequency ‘leaks’ into the neighbouring lines. Measuring a periodic signal over an integer number periods removes the leakage problem completely, and we strongly advise the reader to apply periodic excitation signals whenever it is possible (Pintelon & Schoukens, 2001). However, in many applications the users prefer to apply random noise

excitations for psychological or technological reasons. In this paper we give a new insight in the nature of the leakage errors. The kernel idea is based on the observation that the leakage errors in an FRF measurement are highly structured which allows to split them into two contributions. The first one is due to initial and end condition (transients) effects, the second contributions are due to the interpolation of the transfer function over neighbouring frequency lines. Replacing the rectangular window by the Hanning window shifts the nature of the error from the first contribution to the second one. Explicit expressions will be given to describe this behaviour. Bias and variance expressions are obtained, and the results are illustrated on some simulations.

In the literature a large number of windows are defined and their properties are intensively studied, keeping essentially spectral analysis applications in mind (Harris, 1978). The major contribution of this paper is to study these properties keeping FRF-measurements in mind which leads to new insights, and eventually to the definition of a new window function. This allows to reduce the ‘leakage errors’ on the FRF measurements, while the noise sensitivity is not increased.

<sup>☆</sup> This paper was not presented at any IFAC meeting. This paper was recommended for publication in revised form by Associate Editor Brett Ninness under the direction of Editor Torsten Söderström.

\* Corresponding author.

*E-mail address:* [johan.schoukens@vub.ac.be](mailto:johan.schoukens@vub.ac.be) (J. Schoukens).

An alternative approach to reduce the leakage (and noise) errors is to smooth the FRF over neighbouring lines. This requires again a trade-off between bias (interpolation) errors and variance (leakage or noise). Methods are proposed to do this automatically without user interaction (Stenman & Gustafsson, 2001). However, it is still better to avoid the errors instead of reducing them later on in a smoothing process. And if the variance on the improved measurements is still too high, it is possible to use these as the raw data input to the smoothing algorithms.

## 2. The general framework

### 2.1. Setup

Consider a stable, causal, discrete or continuous time, single-input-single-output (SISO) linear time invariant system  $G$  with impulse response  $g_0$ , and transfer function  $G_0$ ,

$$y(t) = g_0(t) * u_0(t) + v(t) = y_0(t) + v(t), \quad (1)$$

with  $*$  the convolution product,  $u_0$ ,  $y_0$  the exact input and output signal, and  $v(t)$  the disturbing noise.  $N$  samples of the input and output are measured at  $kT_s = k/f_s$ :

$$u_0(k), y(k) \quad \text{with } k = 0, \dots, N-1. \quad (2)$$

The results that are reported in this paper are only valid for stable systems excited with random inputs. This is precisely described in the system and excitation assumptions below.

*Assumption 1. System:* The system  $G$  with impulse response  $g_0(t)$  is assumed to be stable such that  $|g_0(t)| \leq \alpha_1 e^{-\beta_1 t}$  for  $t$ ,  $\alpha_1, \beta_1 > 0$ ; and causal such that  $g_0(t < 0) = 0$ .

*Assumption 2. Excitation:* The excitation is a filtered white noise sequence:  $u_0(t) = f(t) * \rho(t)$ , where  $\rho(t)$  is an i.i.d. random signal with bounded moments of order 4, and  $|f(t)| \leq \alpha_2 e^{-\beta_2 t}$  for  $t$ ,  $\alpha_2, \beta_2 > 0$ .

For continuous time systems, the power spectrum  $S_{u_0 u_0}(\omega)$  is band limited:  $S_{u_0 u_0}(|\omega| > \pi f_s) = 0$ .

In practice the band limited assumption is approximately realized by applying anti-alias filters before sampling the input and output. This is necessary in order to avoid alias errors.

Under Assumption 2, it can be shown that the discrete Fourier transform of  $u_0(t)$  as defined later in (3) will be asymptotically (for  $N \rightarrow \infty$ ) circular complex normally distributed. Moreover, the spectrum  $U_0(k)$  becomes asymptotically independent from  $U_0(l)$  for  $k \neq l$  (Brillinger, 1981; Pintelon & Schoukens, 2001).

*Assumption 3. Disturbing noise:*  $v(t)$  is a stationary noise sequence with bounded second order moments.

### 2.2. The hidden nature of leakage errors in FRF measurements

Starting from measurements (2), the FRF  $G_0(\Omega_l)$  has to be retrieved at the frequencies  $f_l = lf_s/N$ ,  $l = 0, \dots, N/2$ , with  $G_0(\Omega)$  the Fourier transform of the impulse response  $g_0(t)$ , and  $\Omega_l = j2\pi f_l$  for continuous time systems, and  $\Omega_l = e^{j2\pi f_l/f_s}$  for discrete time systems. To solve this problem, the discrete

Fourier transform  $U_0(l)$ ,  $Y(l)$  of the measured input and output signal is calculated, implemented using the fast Fourier transform (FFT) (Brigham, 1974):

$$X(l) = \frac{1}{N} \sum_{k=0}^{N-1} x(k) e^{-j(2\pi/N)kl}. \quad (3)$$

In Pintelon, Schoukens, and Vanderstreen, 1997 and Pintelon and Schoukens, 2001, it is shown for SISO-systems that the following remarkably simple relation holds:

$$\begin{aligned} Y_0(l) &= G_0(\Omega_l)U_0(l) + \tilde{T}_0(\Omega_l) + \Delta_c(\Omega_l) \\ &= G_0(\Omega_l)U_0(l) + T_0(\Omega_l), \end{aligned} \quad (4)$$

with  $G_0$  and  $\tilde{T}_0$  smooth rational functions of the frequency  $\Omega$ .  $\tilde{T}_0$  can be interpreted as a generalized transient term combining initial and end effects. This relation was later generalized to multiple-input-multiple-output systems (McKelvey, 2000).  $\Delta_c(\Omega_l)$  is only present for continuous time systems, it is a residual spectral alias error (see Appendix B) that is a smooth function of  $\Omega$ . From here on we will call  $T_0(\Omega_l) = \tilde{T}_0(\Omega_l) + \Delta_c(\Omega_l)$  the ‘transient term’. With the DFT definition (3),  $U_0(l)$ ,  $Y_0(l)$ ,  $V(l)$  are an  $O(N^{-1/2})$ , and the transient  $T_0(\Omega_l)$  is an  $O(N^{-1})$  (Pintelon & Schoukens, 2001). The impact of initial condition effects on FRF measurements was already recognized before by Douce and Balmer (1985), who studied the contribution to bias errors on the FRF.

If no averaging is applied, and assuming that the disturbing noise  $v(t) = 0$  the estimate of the FRF is given by

$$\hat{G}(\Omega_l) = \frac{Y_0(l)}{U_0(l)} = G_0(\Omega_l) + \frac{T_0(\Omega_l)}{U_0(l)}. \quad (5)$$

It is the last term in (5) that causes the leakage in the FRF measurements and due to the presence of the random variable  $U_0(l)$ , the smooth behaviour of the leakage generating mechanism (the transient  $T_0$ ) is completely lost in the final error on the FRF. However, this hides a highly structured nature that can be described by a smooth function  $T_0$  in  $\Omega$ . Windowing methods exploit this smooth behaviour of  $T_0$  to reduce the leakage errors. Note that the leakage errors in (5) disappear as an  $O(N^{-1/2})$ .

It is common practice to average the estimate  $\hat{G}(\Omega_l)$  over multiple measurements, because for a single realization of the input,  $U_0(l)$  can be very small at some frequencies which makes the FRF estimates extremely sensitive to leakage and noise disturbances resulting in ‘spiky’ measurements. Classically the average is made as (Bendat & Piersol, 1980)

$$\hat{G}^M(\Omega_l) = \frac{\sum_{m=1}^M Y^{[m]}(l) \overline{U_0^{[m]}(l)}}{\sum_{m=1}^M U_0^{[m]}(l) \overline{U_0^{[m]}(l)}}, \quad (6)$$

where  $X^{[m]}(l)$  is the spectrum of the signal in the  $m$ th realization of the experiment. This estimate converges for  $M \rightarrow \infty$  to the noise free solution ( $v(t) = 0$ ) if the output noise  $v(t)$  is not correlated with the input  $u_0(t)$ . But due to the leakage effects,

this limit is still biased:

$$\lim_{m \rightarrow \infty} \hat{G}^M(\Omega_l) = \frac{\lim_{M \rightarrow \infty} \sum_{m=1}^M Y_0^{[m]}(l) \bar{U}_0^{[m]}(l)}{\lim_{M \rightarrow \infty} \sum_{m=1}^M U_0^{[m]}(l) \bar{U}_0^{[m]}(l)} \neq G_0(\Omega_l). \quad (7)$$

### 2.3. Windows

The Fourier transform of a discrete time signal  $x(t)$  is an infinite sum  $\sum_{t=-\infty}^{\infty} x(t)e^{-j\omega t}$ . For engineering applications, this infinite sum should be restricted to a finite one. This is done by considering only a finite number of samples: the sum is calculated on the ‘windowed’ signal,

$$x_w(t) = w(t)x(t), \quad (8)$$

with  $w(t)=0$  if  $t$  is outside the interval  $[0, N-1]$ . A large number of different windows is proposed in the literature (Harris, 1978), here we focus on the rectangular and the Hann window (mostly called Hanning window).

Rectangular (Dirichlet) window:

$$w(t) = 1 \quad \text{for } t = 0, 1, \dots, N-1, \quad (9)$$

Hanning window:

$$w(t) = 0.5 - 0.5 \cos(2\pi t/N). \quad (10)$$

There exists a simple relation between the DFT spectra obtained with the Hanning window ( $X_{\text{Hann}}$ ) and the rectangular window ( $X_{\text{Rect}}$ ) (Harris, 1978):

$$X_{\text{Hann}}(l) = 0.5 \left[ X_{\text{Rect}}(l) - \frac{X_{\text{Rect}}(l-1) + X_{\text{Rect}}(l+1)}{2} \right]. \quad (11)$$

## 3. Analysis of the leakage error

From (4) it is seen that the leakage errors in an FRF measurement are due to the presence of the transient term  $T_0(\Omega)$ . Since this is a smooth function, it can be assumed that it varies ‘slowly’ over neighbouring frequencies, and that information can be used to reduce its impact by averaging the DFT spectra  $U_0(l)$ ,  $Y_0(l)$  over well-chosen combinations of the corresponding spectral input/output lines (this is the frequency domain interpretation of windowing in the time domain). This will work indeed, but the ‘averaging’ process over these neighbouring lines creates a new interpolation error because also  $G_0$  is frequency dependent. The error due to the transient term (the leakage generating mechanism) will be called  $e_1$ , the error due to the ‘interpolation’ of  $G_0$  over neighbouring lines will be called  $e_2$ .

In the subsections below the rectangular and the Hanning window will be analysed. Next, a new window is proposed that has slightly better characteristics and actually can replace the Hanning window as the default choice in practice. During these discussions it is assumed that the disturbing noise  $v(t) = 0$ . At the end the impact of the disturbing noise is analysed for the three proposed windows.

### 3.1. Rectangular window

Using the rectangular window in the FFTs (Bendat & Piersol, 1980; Brigham, 1974), it is found immediately that in the noiseless case

$$\begin{aligned} \hat{G}_{\text{Rect}}(\Omega_l) &= \frac{Y_0(l)}{U_0(l)} = \frac{G_0(\Omega_l)U_0(l)}{U_0(l)} + \frac{T_0(l)}{U_0(l)} \\ &= G_0(\Omega_l) + O(N^{-1/2}) = G_0(\Omega_l) + e_{1\text{Rect}}(l). \end{aligned} \quad (12)$$

In this case no averaging over neighboring lines is done and hence  $e_{2\text{Rect}}(l) = 0$ . This result shows that the leakage errors disappear as an  $O(N^{-1/2})$  for stationary random excitations, which is in agreement with the results of Ljung (1999). The averaged estimate is

$$\begin{aligned} \hat{G}_{\text{Rect}}^M(\Omega_l) &= \frac{\sum_{m=1}^M Y_0^{[m]}(l) \bar{U}_0^{[m]}(l)}{\sum_{m=1}^M U_0^{[m]}(l) \bar{U}_0^{[m]}(l)} = G_0(\Omega_l) \\ &+ \frac{(1/M) \sum_{m=1}^M \bar{U}_0^{[m]}(l) T_0^{[m]}(\Omega_l)}{(1/M) \sum_{m=1}^M U_0^{[m]}(l) \bar{U}_0^{[m]}(l)}. \end{aligned} \quad (13)$$

#### 3.1.1. Systematic contributions

In this section we analyse the systematic error that remains if  $M \rightarrow \infty$ .  $T_0^{[m]}$  is the sum of two transient contributions (at the beginning and the end of the window) and the alias term. Each of these contributions depends on the input signal ( $u(t)$ ,  $t < 0$  for the begin transient;  $u(N-t)$ ,  $t > 0$  for the end transient;  $u(t)$ ,  $t = 0, 1, \dots, N-1$  for the alias term). Hence, a weak correlation between  $T_0^{[m]}(\Omega_l)$  and  $U_0^{[m]}$  exists. It is shown in Appendix A (discrete time systems) and Appendix B (continuous time systems) that this results eventually in a systematic error contribution that can be bounded:

$$\begin{aligned} \lim_{M \rightarrow \infty} \frac{\sum_{m=1}^M \bar{U}_0^{[m]}(l) T_0^{[m]}(\Omega_l)}{\sum_{m=1}^M U_0^{[m]}(l) \bar{U}_0^{[m]}(l)} \\ = \frac{E\{\bar{U}_0^{[m]}(l) T_0^{[m]}(\Omega_l)\}}{E\{U_0^{[m]}(l) \bar{U}_0^{[m]}(l)\}} = O(N^{-1}), \end{aligned} \quad (14)$$

at all excited frequencies ( $E\{U_0^{[m]}(l) \bar{U}_0^{[m]}(l)\} \neq 0$ ),

$$\lim_{M \rightarrow \infty} \hat{G}_{\text{Rect}}^M(\Omega_l) = G_0(\Omega_l) + O(N^{-1}). \quad (15)$$

#### 3.1.2. Variance

In the absence of disturbing noise, the variance of  $\hat{G}_{\text{Rect}}^M(\Omega_l)$  is completely set by the variance of

$$e_{1\text{Rect}}(l) = \frac{(1/M) \sum_{m=1}^M \bar{U}_0^{[m]}(l) T_0^{[m]}(\Omega_l)}{(1/M) \sum_{m=1}^M U_0^{[m]}(l) \bar{U}_0^{[m]}(l)}. \quad (16)$$

In Appendix A, it is shown that the variance of  $e_{1\text{Rect}}(l)$  is bounded by an  $O(M^{-1}N^{-1})$  under Assumptions 1 and 2.

### 3.2. Hanning window

The errors for the rectangular window are completely due to the leakage term  $T_0(l)/U_0(l)$ . An attempt to reduce the impact

of this term is to apply a Hanning window during the calculation of the DFT spectra. From (11) it follows that

$$\hat{G}_{\text{Hann}}(l) = \frac{Y_{0\text{Hann}}(l)}{U_{0\text{Hann}}(l)} = \frac{2Y_0(l) - Y_0(l+1) - Y_0(l-1)}{2U_0(l) - U_0(l+1) - U_0(l-1)}. \quad (17)$$

Define  $\Delta = f_s/N$ . Because  $G_0$  and  $T_0$  are smooth, a Taylor series representation can be used:

$$\begin{aligned} G_0(\Omega_{l\pm 1}) &= G_0(\Omega_l) \pm G_0^{(1)}(\Omega_l)\Delta + G_0^{(2)}(\Omega_l)\frac{\Delta^2}{2} + O(N^{-3}), \\ T_0(\Omega_{l\pm 1}) &= T_0(\Omega_l) \pm T_0^{(1)}(\Omega_l)\Delta + T_0^{(2)}(\Omega_l)\frac{\Delta^2}{2} \\ &\quad + O(N^{-3})O(N^{-1}), \end{aligned} \quad (18)$$

and  $X^{(n)}(\Omega)$  the  $n$ th derivative of  $X(\Omega)$  with respect to  $f = \Omega/(2\pi)$ . The last  $O(N^{-1})$  is because  $T_0^{(3)}$  is an  $O(N^{-1})$ . Substituting (18) in (17) results in

$$\hat{G}_{\text{Hann}}(l) = G_0(\Omega_l) + e_{1\text{Hann}}(l) + e_{2\text{Hann}}(l) + O(N^{-3}) \quad (19)$$

with the leakage error

$$\begin{aligned} e_{1\text{Hann}}(l) &= -T_0^{(2)}(\Omega_l)\Delta^2 \frac{1}{2U_0(l) - U_0(l+1) - U_0(l-1)} \\ &= O(N^{-5/2}), \end{aligned} \quad (20)$$

and the interpolation error

$$\begin{aligned} e_{2\text{Hann}}(l) &= -G_0^{(1)}(\Omega_l)\Delta \frac{U_0(l+1) - U_0(l-1)}{2U_0(l) - U_0(l+1) - U_0(l-1)} \\ &\quad - G_0^{(2)}(\Omega_l)\frac{\Delta^2}{2} \frac{U_0(l+1) + U_0(l-1)}{2U_0(l) - U_0(l+1) - U_0(l-1)} \\ &= O(N^{-1}) + O(N^{-2}). \end{aligned} \quad (21)$$

In this case the leakage error  $e_{1\text{Hann}}$  is reduced to an  $O(N^{-5/2})$ , but compared with the rectangular window a new ‘interpolation’ term  $e_{2\text{Hann}}$  appears which is  $O(N^{-1})$ . Hence, for  $N$  sufficiently large, the Hann window reduces the error from an  $O(N^{-1/2})$  to an  $O(N^{-1})$ , and it switches the nature of the dominant error from ‘leakage’ errors to ‘interpolation’ errors. In the rest of this paper we will always assume that  $N$  is large enough. This aspect will be discussed a bit more in detail in the Conclusions at the end of this section.

Just as for the rectangular window, an averaging procedure is needed:

$$\hat{G}_{\text{Hann}}^M(\Omega_l) = \frac{\sum_{m=1}^M Y_{0\text{Hann}}^{[m]}(l) \overline{U_{0\text{Hann}}^{[m]}(l)}}{\sum_{m=1}^M U_{0\text{Hann}}^{[m]}(l) \overline{U_{0\text{Hann}}^{[m]}(l)}}. \quad (22)$$

### 3.2.1. Systematic contributions

In this subsection we can focus completely on the interpolation error  $e_{2\text{Hann}}$  because this is the dominating term. In Appendix C it is shown that both terms in (21) create a systematic

contribution, and eventually it is found that

$$\begin{aligned} \lim_{M \rightarrow \infty} \hat{G}_{\text{Hann}}^M(\Omega_l) &= G_0(\Omega_l) + 2G_0^{(l)}(\Omega_l) \frac{P_{u_0 u_0}^{(1)}(\Omega_l)}{6P_{u_0 u_0}(\Omega_l)} \Delta^2 \\ &\quad - G_0^{(2)}(\Omega_l) \frac{\Delta^2}{6} \\ &= G_0(\Omega_l) + O(N^{-2}), \end{aligned} \quad (23)$$

with  $P_{u_0 u_0}(\Omega_l) = E\{|U_0(l)|^2\}$ .

Hence compared to the rectangular window, the systematic errors are reduced from  $O(N^{-1})$  to an  $O(N^{-2})$ .

**Remark.** For a white noise excitation,  $P_{u_0 u_0}^{(1)}(\Omega_l) = 0$ .

### 3.2.2. Variance

The variance of  $\hat{G}_{\text{Hann}}^M(\Omega_l)$  is dominated by the first term in (21). In Appendix C it is shown that the variance becomes

$$\text{var}(\hat{G}_{\text{Hann}}^M(\Omega_l)) = \frac{|G_0^{(l)}(\Omega_l)\Delta|^2}{3M} = O(M^{-1}N^{-2}). \quad (24)$$

### 3.2.3. Estimation of the bias and variance

Eqs. (23) and (24) show that it is easy to estimate the level of the systematic errors (for white noise excitation only) and the variance from the available measurement results. Approximating the second derivative of  $G_0$

$$\begin{aligned} G_0^{(2)}(\Omega_l)\Delta^2 &\approx \frac{(2\hat{G}_{\text{Hann}}^M(\Omega_l) - \hat{G}_{\text{Hann}}^M(\Omega_{l-1}) - \hat{G}_{\text{Hann}}^M(\Omega_{l+1}))\Delta^2}{\Delta^2} \\ &= \text{diff}(\text{diff}(\hat{G}_{\text{Hann}}^M(\Omega_{l+1}))) \end{aligned} \quad (25)$$

with  $\text{diff}(X(l)) = X(l+1) - X(l)$ , and using (23) leads to

$$\begin{aligned} \lim_{M \rightarrow \infty} \hat{G}_{\text{Hann}}^M(\Omega_l) - G_0(\Omega_l) &\approx -\frac{\text{diff}(\text{diff}(\hat{G}_{\text{Hann}}^M(\Omega_{l+1})))}{6} \\ \text{if } P_{u_0 u_0}^{(1)}(\Omega_l) &= 0 \quad (\text{white noise excitation}), \end{aligned} \quad (26)$$

and similarly

$$\text{std}(\hat{G}_{\text{Hann}}^M(\Omega_l)) \approx \frac{\text{diff}(\hat{G}_{\text{Hann}}^M(\Omega_{l-1}))}{\sqrt{3M}}. \quad (27)$$

Hence it is possible at the end of a measurement process to quantify very easily the impact of the windowing effects.

### 3.3. The Diff window

The results of Sections 3.1 and 3.2 show that it is possible to reduce the impact of the windowing effects on the FRF-measurements from an  $O(N^{-1})$  to an  $O(N^{-2})$  (systematic error and variance) by replacing the rectangular window by a Hanning window. This explains why the Hanning method became so popular from the very beginning of DFT-based FRF-measurements. However, the study also reveals that this error reduction is obtained due to a shift of the nature of the errors from ‘leakage’ ( $e_1$ ) errors to ‘interpolation’ ( $e_2$ ) errors. The latter grow with the width of the interpolation interval which is

2 bins (3 lines) for the Hanning window. This suggests that it is possible to define an alternative window with a smaller width so that a better balancing between the leakage and interpolation errors is obtained. This idea is elaborated below.

### 3.3.1. A new window

The primary function of the window in an FRF measurement is the suppression of the impact of the transient in (4) while keeping at the same time the interpolation error on the first term in (4) small. An alternative for the 3-lines Hanning window is to consider the difference of the output spectrum that combines only 2 lines:

$$\hat{G}_{\text{Diff}}(\Omega_{l+1/2}) = \frac{Y_0(l+1) - Y_0(l)}{U_0(l+1) - U_0(l)} = \frac{Y_{0\text{Diff}}(l)}{U_{0\text{Diff}}(l)}, \quad (28)$$

and

$$\hat{G}_{\text{Diff}}^M(\Omega_{l+1/2}) = \frac{\sum_{m=1}^M Y_{0\text{Diff}}^{[m]}(l) \bar{U}_{0\text{Diff}}^{[m]}(l)}{\sum_{m=1}^M U_{0\text{Diff}}^{[m]}(l) \bar{U}_{0\text{Diff}}^{[m]}(l)}. \quad (29)$$

Applying again the Taylor series representation (18) but this time around  $\Omega_{l+1/2}$  results in

$$\hat{G}_{\text{Diff}}(\Omega_{l+1/2}) = G_0(\Omega_{l+1/2}) + e_{1\text{Diff}}(l + \frac{1}{2}) + e_{2\text{Diff}}(l + \frac{1}{2}), \quad (30)$$

with leakage error

$$e_{1\text{Diff}}(l + \frac{1}{2}) = T_0^{(1)}(\Omega_{l+1/2}) \Delta \frac{1}{U_0(l+1) - U_0(l)} = O(N^{-3/2}), \quad (31)$$

and interpolation error

$$e_{2\text{Diff}}(l + \frac{1}{2}) = G_0^{(1)}(\Omega_{l+1/2}) \frac{\Delta}{2} \frac{U_0(l+1) + U_0(l)}{U_0(l+1) - U_0(l)} + G_0^{(2)}(\Omega_{l+1/2}) \frac{\Delta^2}{8} = O(N^{-1}) + O(N^{-2}). \quad (32)$$

Note that  $e_{2\text{Diff}}$  is reduced w.r.t.  $e_{2\text{Hann}}$  by working around the middle frequency  $\Omega_{l+1/2}$ . In that case an approximation is made over only half a bin to the left and to the right instead of a full bin for the Hann window. The leakage error is increased to  $O(N^{-3/2})$ , but this is not that important because it is not the dominating error (remember that  $N$  is assumed to be large enough). More detailed results are given in the next section, but first a time domain interpretation is made.

### 3.3.2. Time domain interpretation

Making the difference over two neighboring frequencies can be interpreted as applying the following complex window in the time domain:

$$w(k) = e^{j(2\pi/N)k} - 1, \quad (33)$$

which is shown in Fig. 1.

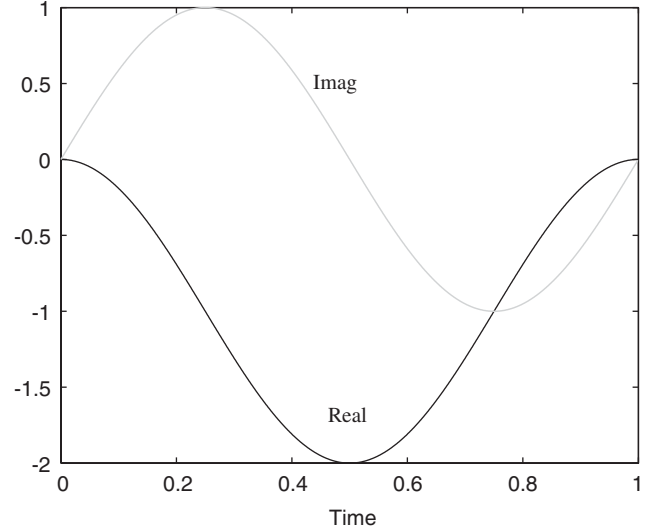


Fig. 1. Real and imaginary parts of the complex window corresponding to the difference operation.

### 3.3.3. Systematic contributions

Although the errors are again dominated by the interpolation error  $e_{2\text{Diff}}$ , it turns out (see Appendix D) that both terms contribute to the limit error with an  $O(N^{-2})$  term

$$\lim_{M \rightarrow \infty} \hat{G}_{\text{Diff}}^M(\Omega_{l+1/2}) = G_0(\Omega_{l+1/2}) + O(N^{-2}). \quad (34)$$

Compared to the rectangular window, the systematic errors are reduced from  $O(N^{-1})$  to an  $O(N^{-2})$ , and the same order is found as for the Hanning window.

### 3.3.4. Variance

The variance of  $G_{\text{Diff}}^M(\Omega_{l+1/2})$  is dominated by the first term in (32). In Appendix D it is shown that the variance becomes

$$\text{var}(\hat{G}_{\text{Diff}}^M(\Omega_{l+1/2})) = \frac{|G_0^{(1)}(\Omega_{l+1/2}) \Delta|^2}{4M} = O(M^{-1}N^{-2}). \quad (35)$$

So the variance is slightly reduced (−1.25 dB) compared to the Hanning window. This allows to reduce the measurement time by 25% for the same level of variance of the leakage error on the measured FRF.

### 3.3.5. Estimation of the bias and variance

Eq. (35) shows that it is easy to estimate the level of the variance from the available measurement results using the same ideas as for the Hanning window:

$$\text{std}(\hat{G}_{\text{Diff}}^M(\Omega_{l+1/2})) = \frac{|\text{diff}(\hat{G}_{\text{Diff}}^M(\Omega_{l+1/2}))|}{\sqrt{4M}}. \quad (36)$$

No expression is given for the limit error, because the systematic transient contributions are not simply described.

## 3.4. Conclusion

In Table 1 all the results of the previous discussions are collected. It is seen that for FRF measurements from records that

Table 1  
Comparison of the Rectangular, Hanning, and Diff windows

Window	Leakage error $e_1$	Interpolation error $e_2$	Systematic error ( $M \rightarrow \infty$ )	Variance
$w_{\text{Rect}}(k) = 1$	$O(N^{-1/2})$	0	$O(N^{-1})$	$O(M^{-1}N^{-1})$
$w_{\text{Hann}}(k) = 0.5 \left(1 - \cos k \frac{2\pi}{N}\right)$	$O(N^{-5/2})$	$O(N^{-1})$	$O(N^{-2})$	$O(M^{-1}N^{-2})$
$w_{\text{Diff}}(k) = 1 - e^{j(2\pi/N)k}$	$O(N^{-3/2})$	$O(N^{-1})$	$O(N^{-2})$	$ G_0^{(1)}(\Omega_l)A ^2/(3M)$ $O(M^{-1}N^{-2})$ $ G_0^{(1)}(\Omega_{l+1/2})A ^2/(4M)$

are sufficiently long, the Hanning window is superior to the rectangular window for a wide range of experimental conditions ( $NT_s$  should be large enough compared to the time constant of the system), while the Diff window even does a little bit better. So the Diff window can replace the Hanning window as default choice in FRF measurements. From the expressions found in this section, it is impossible to say what is the minimum length  $N$  for which the Hanning window is doing better than the rectangular window, or the Diff window is better than the Hanning window. The basic reason for this is that all errors were bounded using expressions of the form  $O(N^{-\alpha})$ , without knowing the exact scale factor that is multiplied with it. It is hard or impossible to give numerical values for this scale factor because it depends on the derivatives  $G_0^{(1)}$ ,  $G_0^{(2)}$ ,  $T_0^{(1)}$ ,  $T_0^{(2)}$ . However, from practical experience it turned out over the years that the required length  $N$  is very low, and from that experience the Hanning window is used nowadays as the default window. Within the same philosophy, the results in Table 1 suggest strongly to replace this ‘classic’ default choice by the Diff window.

#### 4. Noise analysis

The analysis in Section 3 was made assuming that the disturbing noise equals zero. The three windows resulted eventually in the same type of estimates:

$$\hat{G} = \frac{Z}{X_0} = \frac{Z_0 + N_Z}{X_0}, \quad (37)$$

where  $Z$  and  $X$  are defined in Eqs. (12), (17) and (28). For multiple measurements  $Z^{[l]}$ ,  $X^{[l]}$ ,  $l = 1, \dots, M$ , are available, and the  $H_1$  averaging technique is used (Bendat & Piersol, 1980):

$$\hat{G}^M = \frac{\sum_{l=1}^M Z^{[l]} \bar{X}_0^{[l]}}{\sum_{l=1}^M X_0^{[l]} \bar{X}_0^{[l]}}. \quad (38)$$

The variance for  $\hat{G}_{\text{Rect}}^M$ ,  $\hat{G}_{\text{Diff}}^M$ ,  $\hat{G}_{\text{Hann}}^M$  is approximately given by

$$\sigma_G^2 = \frac{\sigma_{N_Z}^2}{ME\{|X|^2\}}. \quad (39)$$

Table 2  
Study of the stochastic behaviour of the averaged spectrum of a random signal

$M$	Additional uncertainty in dB (95% bound)
1	13
2	7.5
4	4.7
8	3.0
16	2.1
32	1.4
64	1.0
128	0.7
256	0.5

This shows that under Assumptions 2 and 3, the noise sensitivity of all these estimators is the same and the variance due to the disturbing noise is

$$\sigma_G^2 = \frac{\sigma_V^2}{ME\{|U_0|^2\}}, \quad (40)$$

with  $E\{\}$  the expected value taken over the successive realizations of the input signal.

For small  $M$ ,  $(1/M)\sum_{l=1}^M |U_0^{[l]}(k)|^2$  can be significantly different from  $E\{|U_0|^2\}$ . At some frequencies large drops in the realized power spectrum appear, jeopardizing the FRF measurement completely. Therefore, it is strongly advised to choose  $M$  large enough to avoid these dips (Pintelon & Schoukens, 2001). In Table 2 the ratio of the 95% lower bound to the rms value is tabulated to illustrate the additional loss in SNR of the weakest components due to the drops in the amplitude spectrum of the individual realizations of the noise excitation. On the average, 5% of the measure frequencies will have a signal-to-noise-ratio (SNR) drop that is larger than the tabulated values.

#### 5. Simulations

The methods that were discussed in the previous section are illustrated on a simulation. A discrete time system (the coefficients are given in Appendix E) is excited with white Gaussian noise (RMS-value of 1).  $M = 64$  experiments of 8192 points are processed, such that 1024 frequency points in the frequency band of interest are available. A first time, no disturbing noise is added ( $v(t) = 0$ ) in order to be able to emphasize the effects that are described in this paper. The simulation is repeated

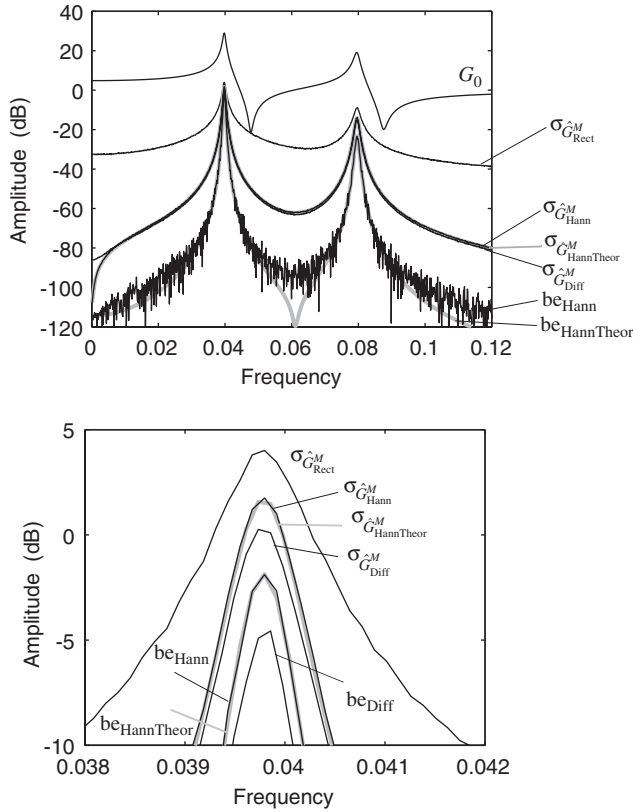


Fig. 2. Comparison of three FRF-estimators:  $G_{\text{Hann}}$ ,  $G_{\text{Diff}}$ ,  $G_{\text{Rect}}$ , together with the exact value  $G_0$  of the FRF. Top: global view; bottom: zoom around the first resonance frequency. The experimental and theoretical standard deviations ( $\sigma$ ) and the bias errors are shown for the Hann ( $\text{be}_{\text{Hann}}$ ) and the Diff windows ( $\text{be}_{\text{Diff}}$ ).

1000 times. The mean and the standard deviation for the three FRF-estimators are calculated and the results are shown in Fig. 2. For the Hanning window, the theoretically predicted and experimentally observed standard deviations are compared and a good agreement is found. This is also true for the systematic error. Note also that the new window does slightly better than the Hanning window as was expected from the theory. A second time, white Gaussian noise is added to the output with an rms-value of 10% of that of the noiseless output. 100 simulations were performed and the standard deviations are shown in Fig. 3. In those frequency regions where the noise dominates the leakage error, the standard deviation of the error is the same for all estimators, as was expected from theory. Note the leakage dominates in a wider region for the rectangular window than for the Hanning and the Diff window. At those frequencies where the leakage error dominates, exactly the same conclusions can be made as in the noiseless simulation.

## 6. Conclusions

In this paper, an analysis of the windowing/leakage effects on FRF-measurements is made. It turns out that the leakage errors in FRF-measurements have hidden a highly structured nature that can be used to reduce their impact. The arguments

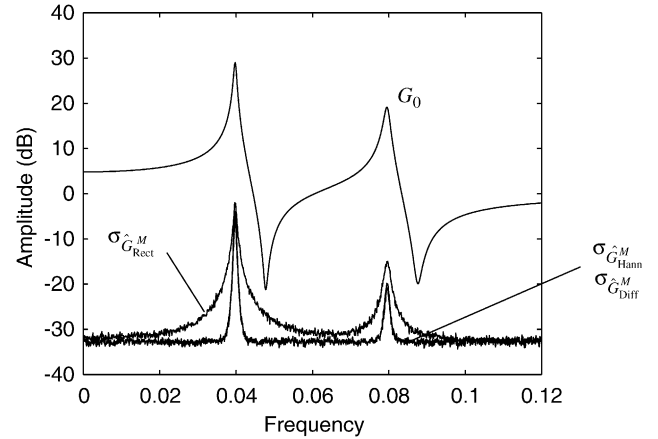


Fig. 3. Comparison of the three FRF-estimators in the presence of output noise:  $G_{\text{Hann}}$ ,  $G_{\text{Diff}}$ ,  $G_{\text{Rect}}$ , together with the exact value  $G_0$  of the FRF.

used in window analysis for spectral analysis applications cannot be unaltered transferred to FRF-measurements. Replacing the rectangular window by alternatives (for example Hanning) shifts the nature of the error from leakage to interpolation. Although the popular Hanning window is also a good choice for FRF-measurements, it turns out that an alternative ‘Diff’ window can be proposed with slightly better properties. This Diff window allows to reduce the required measurement time with 25% if the leakage errors are the dominant error source. If the output noise is the dominating error source, both windows have the same disturbing noise sensitivity. Eventually, simple but accurate expressions to estimate the variance that is induced by the leakage effect are given.

## Acknowledgements

The authors would like to thank Bart De Moor, Michel Gevers, Lennart Ljung, and Paul Van den Hof for the discussions on this topic at the November 2003 meeting.

This work was supported by the FWO, the Flemish government (GOA-ILiNos), and the Belgian government as a part of the Belgian program on Interuniversity Poles of Attraction (IUAP V/22).

## Appendix A. Errors of the rectangular window for discrete time systems

In this appendix we calculate the systematic error and the variance on the FRF due to leakage errors for discrete time systems.

### A.1. Systematic errors

In this section it is shown that

$$\frac{E\{\bar{U}_0^{[m]}(l)T_0^{[m]}(l)\}}{E\{U_0^{[m]}(l)\bar{U}_0^{[m]}(l)\}} = O(N^{-1})$$

at all excited frequencies.

Consider the fundamental expression (4):  $Y_0(l) = G_0(\Omega_l)U_0(l) + T_0(\Omega_l)$  (in this case  $\Delta_c = 0$ ). The structure of  $T_0(\Omega_l)$  is analysed and interpreted in detail by Pintelon and Schoukens (2001, Section 2.6.4 & Appendix 5.B). A possible representation of the transient  $T_0$  is to consider it as the sum of two contributions  $-t_{01}(t) + t_{02}(t)$ . The first term  $t_{01}$  is due to the excitation of the system before the start of the experiment (impact of the initial conditions) and it should be subtracted from the measured output. The second contribution  $t_{02}$  is due to the not measured response of the system once the measurement is stopped and it should be added to the measured output:

$$t_{01}(t) = \sum_{k=-\infty}^{-1} g_0(t-k)u_0(k), \quad t = 0, 1, \dots, N-1, \quad (41)$$

and

$$t_{02}(t) = \sum_{k=0}^{N-1} g_0(t-k)u_0(k), \quad t = N, N+1, \dots, \infty. \quad (42)$$

Consider  $T_0(\Omega_l) = T_{01}(\Omega_l) + T_{02}(\Omega_l)$  with

$$\begin{aligned} T_{01}(\Omega_l) &= \frac{1}{N} \sum_{r=0}^{N-1} t_{01}(r) e^{-j(2\pi/N)rl} \\ &= \frac{1}{N} \sum_{r=0}^{N-1} \sum_{k=-\infty}^{-1} g_0(r-k)u_0(k) e^{-j(2\pi/N)rl}, \\ T_{02}(\Omega_l) &= \frac{1}{N} \sum_{r=N}^{\infty} t_{02}(r) e^{-j(2\pi/N)rl} \\ &= \frac{1}{N} \sum_{r=N}^{\infty} \sum_{k=0}^{N-1} g_0(r-k)u_0(k) e^{-j(2\pi/N)rl}, \end{aligned} \quad (43)$$

and take the expected value after multiplication with  $\bar{U}_0(l) = (1/N) \sum_{s=0}^{N-1} u_0(s) e^{j(2\pi/N)sl}$ . This gives for the first term (the second one is calculated completely similarly)

$$\begin{aligned} &|E\{T_{01}(\Omega_l)\bar{U}_0(l)\}| \\ &= \left| \frac{1}{N^2} \sum_{r=0}^{N-1} \sum_{s=0}^{N-1} \sum_{k=-\infty}^{-1} g_0(r-k) E\{u_0(k) \right. \\ &\quad \times u_0(s)\} e^{-j(2\pi/N)(r-s)l} \Big|. \\ &\leq \frac{1}{N^2} \sum_{r=0}^{N-1} \sum_{s=0}^{N-1} \sum_{k=-\infty}^{-1} |g_0(r-k)| |R_{u_0 u_0}(k-s)|. \end{aligned} \quad (44)$$

From Assumption 2, it follows that

$$|R_{u_0 u_0}(k-s)| \leq \alpha_3 e^{-\beta_2|k-s|} \leq \alpha_3 e^{-\beta_2|k|} e^{-\beta_2 s} \quad (k < 0, s \geq 0), \quad (45)$$

and similarly from Assumption 1,

$$|g_0(r-k)| \leq \alpha_1 e^{-\beta_1|r-k|} \leq \alpha_1 e^{-\beta_1|k|} e^{-\beta_1 r} \quad (k < 0, r \geq 0). \quad (46)$$

Substituting these expressions in the triple sum results eventually in

$$E\{T_{01}(\Omega_l)\bar{U}_0(l)\} = \frac{1}{N^2} O(N^0) = O(N^{-2}). \quad (47)$$

On the other hand, it is clear that

$$\begin{aligned} E\{|U_0(l)|^2\} &= \frac{1}{N^2} \sum_{r=0}^{N-1} \sum_{s=0}^{N-1} E\{u_0(r) e^{-j(2\pi/N)rl} u_0(s) e^{j(2\pi/N)sl}\} \\ &= \frac{1}{N^2} \sum_{r=0}^{N-1} \sum_{s=0}^{N-1} R_{u_0 u_0}(r-s) e^{-j(2\pi/N)(r-s)l}. \end{aligned} \quad (48)$$

Since  $R_{u_0 u_0}$  is exponentially bounded,  $E\{|U_0(l)|^2\} = (1/N^2) O(N) = O(N^{-1})$  at those frequencies where the system is excited. At these frequencies the expected value equals

$$\begin{aligned} \frac{R_{u_0 u_0}(0)}{N} + \frac{2}{N} \sum_{m=1}^{N-1} \left(1 - \frac{m}{N}\right) R_{u_0 u_0}(0) \cos\left(2\pi \frac{ml}{N}\right) \\ = O(N^{-1}). \end{aligned} \quad (49)$$

This estimate of the power spectrum of  $u_0$  is known as Bartlett's method (see, for example, Proakis & Manolakis, 1996). It converges to

$$\begin{aligned} E\{|U_0(l)|^2\} &= P_{u_0 u_0}(\Omega_l) = |F(\Omega_l)|^2 W_B(\Omega_l) \quad \text{with} \\ W_B(\Omega) &= \frac{1}{N} \left( \frac{\sin(N\Omega/2)}{\sin(\Omega/2)} \right)^2, \end{aligned} \quad (50)$$

which is the power spectrum  $|F(\Omega_l)|^2$  calculated with a triangular window.

Combining (47) and (49) proves the appendix.

## A.2. Variance

Notice that

(i)  $U_0^{[m]}, T_0^{[m]}$  is independent  $U_0^{[n]}, T_0^{[n]}$  for  $m \neq n$ .

(ii) Under Assumption 2, the denominator is within a constant  $\chi^2(2M)$  distributed and hence converges to  $E\{|U_0(l)|^2\} = O(N^{-1})$  for growing values of  $M$ . The numerator converges to  $E\{T_{01}(\Omega_l)\bar{U}_0(l)\} = O(N^{-2})$  (47). So  $e_{1\text{Rect}}(l)$  can be written as ( $E\{T_{01}(\Omega_l)\bar{U}_0(l)\} = A_0$ , and  $E\{|U_0(l)|^2\} = B_0$ )

$$\begin{aligned} e_{1\text{Rect}}(l) &= \frac{(1/M) \sum_{m=1}^M \bar{U}_0^{[m]}(l) T_0^{[m]}(\Omega_l)}{(1/M) \sum_{m=1}^M U_0^{[m]}(l) \bar{U}_0^{[m]}(l)} \\ &= \frac{A_0 + a}{B_0 + b} \approx \frac{1}{B_0} \left( A_0 + a - \frac{bA_0}{B_0} \right), \end{aligned} \quad (51)$$

with

$$\frac{A_0}{B_0} \quad \text{an } O(N^{-1}) \quad (\text{see section Systematic errors}). \quad (52)$$

Note also that

$$a \text{ is an } O(N^{-3/2})O(M^{-1/2}), \quad (53)$$

because each term in the sum of  $a$  is an  $O(N^{-3/2})O(M^{-1})$ ,  $E\{a\} = 0$  by definition, and the individual terms in the sum are

independent. Similarly it is found that  $b = O(N^{-1})O(M^{-1/2})$ . Hence  $a$  dominates  $bA_0/B_0$  in (51).

(iii) The variance of  $e_{1\text{Rect}}(l)$  is dominated by  $\text{var}(a)/|B_0|^2$ :

$$\begin{aligned} \text{var}(e_{1\text{Rect}}(l)) &\leq \frac{E\{|a|^2\}}{|B_0|^2} = \frac{O(N^{-3})O(M^{-1})}{O(N^{-2})} \\ &= O(N^{-1}M^{-1}). \end{aligned} \quad (54)$$

**Appendix B. Errors of the rectangular window for continuous time systems**

*B.1. Basic relations*

In this section we consider a causal continuous time system. First we setup the expressions for the continuous input and output signals, considered on the interval  $0 \leq t \leq T = NT_s$ . In order to indicate explicitly the continuous time nature,  $\omega$  is used as frequency variable. Define

$$U_{0T}(\omega) = \frac{1}{T} \int_0^T u_0(t) e^{-j\omega t} dt$$

(windowed Fourier transform),

$$Y_{0T}(\omega) = \frac{1}{T} \int_0^T y_0(t) e^{-j\omega t} dt,$$

$$Y_1(\omega) = \frac{1}{T} \int_0^T \int_{-\infty}^0 g_0(t - \tau) u_0(\tau) e^{-j\omega t} dt d\tau$$

(initial conditions),

$$Y_2(\omega) = \frac{1}{T} \int_T^\infty \int_0^T g_0(t - \tau) u_0(\tau) e^{-j\omega t} dt d\tau$$

(end conditions). (55)

Note that  $Y_1(\omega), Y_2(\omega)$  are smooth (rational) functions of  $\omega$ .

Then the following relation holds:

$$y_0(t) = \int_{-\infty}^0 g_0(t - \tau) u_0(\tau) d\tau + \int_0^t g_0(t - \tau) u_0(\tau) d\tau. \quad (56)$$

$$\begin{aligned} Y_{0T}(\omega) &= \frac{1}{T} \int_0^T y_0(t) e^{-j\omega t} dt \\ &= \frac{1}{T} \int_0^T \left\{ \int_{-\infty}^0 g_0(t - \tau) u_0(\tau) d\tau \right\} e^{-j\omega t} dt \\ &\quad + \frac{1}{T} \int_0^T \left\{ \int_0^t g_0(t - \tau) u_0(\tau) d\tau \right\} e^{-j\omega t} dt \\ &= Y_1(\omega) + \frac{1}{T} \int_0^\infty \left\{ \int_0^t g_0(t - \tau) u_0(\tau) d\tau \right\} e^{-j\omega t} dt \\ &\quad - \frac{1}{T} \int_T^\infty \left\{ \int_0^t g_0(t - \tau) u_0(\tau) d\tau \right\} e^{-j\omega t} dt. \end{aligned} \quad (57)$$

Notice that for a causal system  $\int_0^t g_0(t - \tau) u_0(\tau) d\tau = \int_0^\infty g_0(t - \tau) u_0(\tau) d\tau$ . Moreover, without any loss of generality, it can be assumed that  $u_0(t > T) = 0$ , because for a causal system this

input does not affect the experiment in  $[0, T]$ , which allows to change the integration limits in the last integral. Hence

$$Y_{0T}(\omega) = Y_1(\omega) + \frac{1}{T} \int_0^\infty \left\{ \int_0^\infty g_0(t - \tau) u_0(\tau) d\tau \right\} \times e^{-j\omega t} dt - Y_2(\omega) \quad (58)$$

or

$$Y_{0T}(\omega) = \frac{1}{T} \int_0^\infty \int_0^\infty g_0(t - \tau) u_0(\tau) e^{-j\omega t} dt d\tau + Y_1(\omega) - Y_2(\omega). \quad (59)$$

Keeping in mind that we set  $u_0(t > T) = 0$ , (59) can be rearranged as

$$Y_{0T}(\omega) = G_0(j\omega) U_{0T}(\omega) + Y_1(\omega) - Y_2(\omega). \quad (60)$$

The reader should realize that the spectra in (60) are based on continuous time Fourier transforms. These should be replaced first by the discrete time equivalents. However,  $U_{0T}(\omega), Y_1(\omega), Y_2(\omega)$  are not band limited, even if  $u_0$  is. Hence the DFT spectra will be prone to alias errors, for example

$$Y_{0\text{DFT}}(l) = Y_{0T}(\omega_l) + \sum_{\substack{k \neq 0 \\ k=-\infty}}^{\infty} Y_{0T}(\omega_l + k\omega_s)$$

with

$$\omega_s = 2\pi/T_s, \quad (61)$$

and similar for the other spectra. Eventually, (60) becomes

$$\begin{aligned} Y_{0\text{DFT}}(l) &= G_0(j\omega_l) U_{0\text{DFT}}(l) + Y_{1\text{DFT}}(k) - Y_{2\text{DFT}}(l) \\ &\quad + \sum_{\substack{k \neq 0 \\ k=-\infty}}^{\infty} (G_0(j(\omega_l - k\omega_s)) \\ &\quad - G_0(j\omega_l)) U_{0T}(\omega_l + k\omega_s) \\ &= G_0(j\omega_l) U_{0\text{DFT}}(l) + Y_{1\text{DFT}}(l) \\ &\quad - Y_{2\text{DFT}}(l) + \Delta_c(l). \end{aligned} \quad (62)$$

From Pintelon and Schoukens (2001, Appendix 5.F.2 of Chapter 5) it follows that  $\Delta_c(l)$  is an  $O(N^{-1})$  for the DFT definition (3).

*B.2. Systematic errors*

For the systematic errors, the cross-correlation between  $U_{0\text{DFT}}(l)$  and  $Y_{1\text{DFT}}(l), Y_{2\text{DFT}}(l)$ , or  $\Delta_c(l)$  is needed.

First  $E\{Y_{1\text{DFT}}(l) \bar{U}_{0\text{DFT}}(l)\}$  is considered, next  $E\{\Delta_c(l) \bar{U}_{0\text{DFT}}(l)\}$  is analysed.

(i)  $E\{Y_{1\text{DFT}}(l) \bar{U}_{0\text{DFT}}(l)\}$  (similar for  $E\{Y_{2\text{DFT}}(l) \bar{U}_{0\text{DFT}}(l)\}$ )

$$\begin{aligned} E\{Y_{1\text{DFT}}(l) \bar{U}_{0\text{DFT}}(l)\} &= \frac{1}{N^2} \sum_{r=0}^{N-1} \int_{-\infty}^0 \sum_{s=0}^{N-1} g_0(rT_s - \tau) \\ &\quad \times R_{u_0 u_0}(sT_s - \tau) e^{-j(2\pi/N)lr} e^{j(2\pi/N)ls} d\tau, \end{aligned} \quad (63)$$

and

$$|E\{Y_{1\text{DFT}}(l)\overline{U}_{0\text{DFT}}(l)\}| \leq \frac{1}{N^2} \sum_{r=0}^{N-1} \int_{-\infty}^0 \sum_{s=0}^{N-1} |g_0(rT_s - \tau)| \times |R_{u_0 u_0}(sT_s - \tau)| d\tau. \quad (64)$$

From Assumption 1, it is known that  $|g_0(t)|$  is exponentially bounded as function of time and hence

$$|g_0(rT_s - \tau)|_{T_s} \leq \int_{(r-1)T_s}^{rT_s} \alpha_1 e^{-\beta_1 t_1} dt_1 \leq e^{\beta_1 T_s} \int_{rT_s}^{(r+1)T_s} \alpha_1 e^{-\beta_1 t_1} dt_1. \quad (65)$$

A similar result is found for the second sum using Assumption 2. So

$$|E\{Y_{1\text{DFT}}(l)\overline{U}_{0\text{DFT}}(l)\}| \leq \frac{e^{\beta_1 T_s} e^{\beta_2 T_s}}{N^2 T_s^2} \int_0^T \int_{-\infty}^0 \int_0^T \alpha_1 e^{-\beta_1 t_1} \alpha_3 e^{-\beta_2(t_2 - \tau)} \times dt_1 d\tau dt_2 \leq T_s^{-2} O(N^{-2}). \quad (66)$$

$$e_{21\text{Hann}}^M(l) = -G_0^{(1)}(\Omega_l) \Delta \frac{(1/M) \sum_{m=1}^M (U_0^{[m]}(l+1) - U_0^{[m]}(l-1))(2\overline{U}_0^{[m]}(l) - \overline{U}_0^{[m]}(l+1) - \overline{U}_0^{[m]}(l-1))}{(1/M) \sum_{m=1}^M |2U_0^{[m]}(l) - U_0^{[m]}(l+1) - U_0^{[m]}(l-1)|^2}. \quad (72)$$

So, for a given sampling frequency  $f_s = 1/T_s$ , it follows that for a continuous time system with sampled input/output data

$$|E\{Y_{1\text{DFT}}(l)\overline{U}_{0\text{DFT}}(l)\}| = O(N^{-2}). \quad (67)$$

$$(ii) E\{\Delta_c(l)\overline{U}_{0\text{DFT}}(l)\}$$

$$U_{0\text{DFT}}(l) = U_{0T}(\omega_l) + \sum_{\substack{k \neq 0 \\ k=-\infty}}^{\infty} U_{0T}(\omega_l + k\omega_s) = U_{0T}(\omega_l) + \Delta_U(l). \quad (68)$$

Note that  $U_{0T}(\omega_l)$  is an  $O(N^{-1/2})$  and  $\Delta_U(l)$  is an  $O(N^{-1})$ . So

$$E\{\Delta_c(l)\overline{\Delta_U}(\omega_l)\} \leq O(N^{-2}), \quad (69)$$

and only  $E\{\Delta_c(l)\overline{U}_{0T}(\omega_l)\}$  remains to be analysed, this is in essence the correlation between  $U_{0T}(\omega_l)$  and the sum of all aliased contributions  $U_{0T}(\omega_l + k\omega_s)$ . After some tedious calculations (Schoukens, 2004), it turns out that

$$E\{\Delta_c(l)\overline{U}_{0T}(\omega_l)\} = O(N^{-2}) \quad \text{and hence } E\{\Delta_c(l)\overline{U}_0(\omega_l)\} = O(N^{-2}). \quad (70)$$

Starting from (67), (69), and (70), expression (14) can be proven again but this time for sampled data measured on continuous time systems, using the proof for the discrete time systems.

### B.3. Variance errors

The results of the discrete system in Appendix A, apply directly to the continuous system using (67), (69), and (70) instead of (47).

## Appendix C. Errors of the Hanning method

In this section the systematic error and the variance of  $e_{1\text{Hann}} + e_{2\text{Hann}}$  is analysed. The proofs are valid for discrete and continuous time systems. Because  $e_{1\text{Hann}}$  is an  $O(N^{-5/2})$ , the Hanning error is completely dominated by  $e_{2\text{Hann}}$ :

$$e_{2\text{Hann}} = -G_0^{(1)}(\Omega_l) \Delta \frac{U_0(l+1) - U_0(l-1)}{2U_0(l) - U_0(l+1) - U_0(l-1)} - G_0^{(2)}(\Omega_l) \frac{\Delta^2}{2} \frac{U_0(l+1) + U_0(l-1)}{2U_0(l) - U_0(l+1) - U_0(l-1)} = e_{21\text{Hann}} + e_{22\text{Hann}} = O(N^{-1}) + O(N^{-2}). \quad (71)$$

### C.1. Systematic error

The limit value for  $e_{21\text{Hann}}$  and  $e_{22\text{Hann}}$  are analysed for the number of averages  $M \rightarrow \infty$ , using (22),

$$(1) \lim_{M \rightarrow \infty} e_{21\text{Hann}}^M$$

Notice that under Assumption 2 for  $N \rightarrow \infty$ ,  $E\{U_0^{[m]}(l_1)U_0^{[m]}(l_2)\} = 0$  ( $l_1 \neq l_2$ ). Using (50), it follows that

$$\lim_{M \rightarrow \infty} e_{21\text{Hann}} = -G_0^{(1)}(\Omega_l) \Delta \frac{P_{u_0 u_0}(\Omega_{l-1}) - P_{u_0 u_0}(\Omega_{l+1})}{4P_{u_0 u_0}(\Omega_l) + P_{u_0 u_0}(\Omega_{l-1}) + P_{u_0 u_0}(\Omega_{l+1})} \approx -2G_0^{(1)}(\Omega_l) \Delta \frac{P_{u_0 u_0}^{(1)}(\Omega_l) \Delta}{6P_{u_0 u_0}(\Omega_l)} \quad (73)$$

or

$$\lim_{M \rightarrow \infty} e_{21\text{Hann}} \approx 2G_0^{(1)}(\Omega_l) \frac{P_{u_0 u_0}^{(1)}(\Omega_l)}{6P_{u_0 u_0}(\Omega_l)} \Delta^2. \quad (74)$$

$$(2) \lim_{M \rightarrow \infty} e_{22\text{Hann}}^M$$

$$\lim_{M \rightarrow \infty} e_{22\text{Hann}}^M = -G_0^{(2)}(\Omega_l) \frac{\Delta^2}{2} \times \frac{E\{|U_0(l+1)|^2 + |U_0(l-1)|^2\}}{4E\{|U_0(l)|^2\} + E\{|U_0(l+1)|^2 + |U_0(l-1)|^2\}} \approx -G_0^{(2)}(\Omega_l) \frac{\Delta^2}{6}. \quad (75)$$

Combining both results leads immediately to

$$\lim_{M \rightarrow \infty} e_{2\text{Hann}}^M \approx -2G_0^{(1)}(\Omega_l) \frac{P_{u_0 u_0}^{(1)}(\Omega_l)}{6P_{u_0 u_0}(\Omega_l)} \Delta^2 - G_0^{(2)}(\Omega_l) \frac{\Delta^2}{6} = O(N^{-2}). \quad (76)$$

### C.2. Variance

The variance of  $e_{2\text{Hann}}$  is completely dominated by  $e_{21\text{Hann}}$  which is an  $O(N^{-1})$ . Similar to the variance calculations for the rectangular window in Appendix A, it is set also here by the variance of the numerator of the fraction  $B/A$  in (72). The numerator  $B$  consists of terms of order  $O(N^{-1})$ , while its mean value is an  $O(N^{-2})$ . Hence  $\text{var}(B) \approx E\{|B|^2\}$ . The calculation of this expected value is significantly simplified by noticing that  $U_0$  is (i) asymptotically circular complex normally distributed for  $N \rightarrow \infty$ ; (ii) independent over the different realizations of the input; (iii) independent over the frequency. This results eventually in

$$\begin{aligned} & \frac{1}{M^2} \sum_{m=1}^M E\{|U_0^{[m]}(l+1) - U_0^{[m]}(l-1)|^2 |2\bar{U}_0^{[m]}(l) \\ & - \bar{U}_0^{[m]}(l+1) - \bar{U}_0^{[m]}(l-1)|^2\} \\ & \approx \frac{12}{M} E\{|U_0(l)|^2\}, \end{aligned} \quad (77)$$

and

$$\sigma_{e_{2\text{Hann}}^M}^2(l) \approx \frac{|G_0^{(1)}(\Omega_l)|^2 |\Delta|^2}{3M}. \quad (78)$$

### Appendix D. Errors of the Diff method

In this section the systematic error and the variance of  $e_{1\text{Diff}}$  +  $e_{2\text{Diff}}$  is analysed. The proofs are valid for discrete and continuous time systems.

#### D.1. Systematic error

In this section, the errors are analysed for the number of averages  $M \rightarrow \infty$ , using (28)

$$(1) \lim_{M \rightarrow \infty} e_{1\text{Diff}}^{[m]}(l).$$

From (47) it follows that

$$\begin{aligned} e_{1\text{Diff}}^{[m]}(l) &= \Delta \frac{\sum_{m=1}^M T_0^{(1)}(\Omega_{l+1/2})(\bar{U}_0^{[m]}(l+1) - \bar{U}_0^{[m]}(l))}{\sum_{m=1}^M |U_0^{[m]}(l+1) - U_0^{[m]}(l)|^2} \\ &= O(N^{-1}) \frac{O(N^{-2})}{O(N^{-1})} = O(N^{-2}). \end{aligned} \quad (79)$$

$$(2) \lim_{M \rightarrow \infty} e_{2\text{Diff}}^{[m]}(l).$$

Consider

$$\begin{aligned} e_{2\text{Diff}}(l) &= -G_0^{(1)}(\Omega_l) \frac{\Delta}{2} \frac{U_0(l+1) + U_0(l)}{U_0(l+1) - U_0(l)} - G_0^{(2)}(\Omega_l) \frac{\Delta^2}{8} \\ &= e_{21\text{Diff}}(l) + e_{22\text{Diff}}(l) \\ &= O(N^{-1}) + O(N^{-2}), \end{aligned} \quad (80)$$

$$e_{21\text{Diff}}^m(l) = -G_0^{(1)}(\Omega_l) \frac{\Delta}{2} \frac{(1/M) \sum_{m=1}^M (U_0^{[m]}(l+1) + U_0^{[m]}(l)) (\bar{U}_0^{[m]}(l+1) - \bar{U}_0^{[m]}(l))}{(1/M) \sum_{m=1}^M |U_0^{[m]}(l+1) - U_0^{[m]}(l)|^2}. \quad (81)$$

Similar to the previous appendix, it follows that for  $M \rightarrow \infty$

$$\begin{aligned} \lim_{M \rightarrow \infty} e_{21\text{Diff}}^M &= -G_0^{(1)}(\Omega_l) \Delta \frac{P_{u_0 u_0}^{(1)}(\Omega_l) \Delta}{P_{u_0 u_0}(\Omega_l)} \\ &= O(N^{-2}), \end{aligned} \quad (82)$$

$e_{22\text{Diff}}$  is independent of  $M$ , and hence its limiting value equals  $-G_0^{(2)}(\Omega_l)(\Delta^2/8) = O(N^{-2})$ .

Bringing the three sub-results together leads to

$$\lim_{M \rightarrow \infty} e_{2\text{Diff}}^M = O(N^{-2}). \quad (83)$$

#### D.2. Variance

Because  $e_{1\text{Diff}}$  is an  $O(N^{-3/2})$ , the Diff variance is completely dominated by  $e_{2\text{Diff}}$ .

The variance of  $e_{2\text{Diff}}$  is completely dominated by  $e_{21\text{Diff}}$  which is an  $O(N^{-1})$ . The denominator in (81) converges to a constant

$$\lim_{M \rightarrow \infty} \frac{1}{M} \sum_{m=1}^M |U_0^{[m]}(l+1) - U_0^{[m]}(l)|^2 \approx \frac{2E\{|U_0(l)|^2\}}{M}. \quad (84)$$

Hence, similar to Appendix A, the variance is set by the variance of the numerator which is given in this case (similar to Appendix C) by

$$\begin{aligned} & \frac{1}{M^2} \sum_{m=1}^M E\{|U_0^{[m]}(l+1) + U_0^{[m]}(l)|^2 |\bar{U}_0^{[m]}(l+1) - \bar{U}_0^{[m]}(l)|^2\} \\ & \approx \frac{4}{M} E\{|U_0(l)|^2\}. \end{aligned} \quad (85)$$

and

$$\sigma_{e_{2\text{Diff}}^M}^2(l) \approx \frac{|G_0^{(1)}(\Omega_l)|^2 |\Delta|^2}{4M}. \quad (86)$$

### Appendix E

The coefficients of the  $A$  and  $B$  polynomials of the system  $G_0(z^{-1}) = B(z^{-1})/A(z^{-1})$  used in the simulation are given by

$$\begin{aligned} \mathbf{b} &= [-9.468\text{e} - 002 \quad 3.409\text{e} - 001 \quad -4.936\text{e} - 001 \\ & \quad 3.380\text{e} - 001 \quad -9.308\text{e} - 002], \end{aligned}$$

$$\begin{aligned} \mathbf{a} &= [-9.395\text{e} - 002 \quad 3.457\text{e} - 001 \quad -5.0367\text{e} - 001 \\ & \quad 3.431\text{e} - 001 \quad -9.255\text{e} - 002]. \end{aligned}$$

### References

- Bendat, J. S., & Piersol, A. G. (1980). *Engineering applications of correlations and spectral analysis*. New York: Wiley.
- Brigham, E. O. (1974). *The fast Fourier transform*. New Jersey, USA: Prentice-Hall.

- Brillinger, D. R. (1981). *Time series: Data analysis and theory*. New York: McGraw-Hill.
- Douce, J. L., & Balmer, L. (1985). Transient effects in spectrum estimation. *IEE proceedings*, Vol. 132. Pt. D, No. 1 (pp. 25–29).
- Harris, F. J. (1978). On the use of windows for harmonic analysis with discrete Fourier transform. *Proceedings of the IEEE*, Vol. 66 (pp. 51–83).
- Ljung, L. (1999). *System identification. Theory for the user*. New Jersey, USA: Prentice-Hall.
- McKelvey, T. (2000). Frequency domain identification. *IFAC SYSID 2000 symposium on system identification*. Santa Barbara, California, June 21–23.
- Pintelon, R., & Schoukens, J. (2001). *System identification. A frequency domain approach*. New York: IEEE press and Wiley.
- Pintelon, R., Schoukens, J., & Vanderstreen, G. (1997). Frequency-domain identification using arbitrary signals. *IEEE Transactions on Automatic Control*, 42, 1717–1720.
- Proakis, J. G., & Manolakis, D. G. (1996). *Digital signal processing*. New Jersey, USA: Prentice-Hall.
- Schoukens, J. (2004). Correlation of aliased Fourier coefficients. *Internal Note VUB-ELEC-June 2004*.
- Stenman, A., & Gustafsson, F. (2001). Adaptive smoothing methods for frequency-function estimation. *Automatica*, 37, 675–685.



**Yves Rolain** is with the Electrical Measurement Department (ELEC), Vrije Universiteit Brussel (VUB), Brussels, Belgium. His main research interests are non-linear microwave measurement techniques, applied digital signal processing, parameter estimation/system identification, and biological agriculture.



**Rik Pintelon** received the degree of engineer in 1982, the degree of doctor in applied science in 1988, all from the Vrije Universiteit Brussel (VUB), Brussels, Belgium. He is presently a professor at the VUB in the Electrical Measurement Department (ELEC). His main research interests are in the field of parameter estimation/system identification, and signal processing.



**Johan Schoukens** received the degree of engineer in 1980, the degree of doctor in applied sciences in 1985, all from the Vrije Universiteit Brussel (VUB). He is presently a professor at the VUB. The prime factors of his research are in the field of system identification for linear and non-linear systems, and growing tomatoes and melons in his greenhouse.